

Uniaxial dielectric mediums with hyperbolic dispersion relations

Tom G. Mackay^{*}

School of Mathematics, University of Edinburgh, Edinburgh EH9 3JZ, UK

Akhlesh Lakhtakia[†]

*CATMAS — Computational & Theoretical Materials Sciences Group
Department of Engineering Science and Mechanics
Pennsylvania State University, University Park, PA 16802–6812, USA*

Ricardo A. Depine[‡]

*Grupo de Electromagnetismo Aplicado, Departamento de Física,
Facultad de Ciencias Exactas y Naturales, Universidad de Buenos Aires,
Ciudad Universitaria, Pabellón I, 1428 Buenos Aires, Argentina*

Abstract

The dispersion relations for conventional uniaxial dielectric mediums may be characterized as elliptical or elliptical-like, according to whether the medium is nondissipative or dissipative, respectively. However, under certain constitutive parameter regimes, the dispersion relations may be hyperbolic or hyperbolic-like. We investigate planewave propagation in a hyperbolic/hyperbolic-like uniaxial dielectric medium. For both evanescent and nonevanescent propagation, the phase velocity is found to be positive with respect to the time-averaged Poynting vector. A conceptualization of a hyperbolic-like uniaxial medium as a homogenized composite medium is presented.

Keywords: Hyperbolic dispersion relations, elliptical dispersion relations, Bruggeman homogenization formalism

1 Introduction

As the materials sciences and technologies continue their rapid development, realistic possibilities are emerging of realizing so-called *metamaterials* with novel and hitherto unconsidered optical/electromagnetic properties. A prime example is provided by the recently

^{*}Corresponding author. E-mail: T.Mackay@ed.ac.uk

[†]E-mail: akhlesh@psu.edu; also affiliated with Department of Physics, Imperial College, London SW7 2BZ, UK

[‡]E-mail: rdep@df.uba.ar

discovered metamaterials which support planewave propagation with *negative phase velocity* (NPV), and thereby negative refraction. Until 2000, little attention had been paid to the phenomenon of negative refraction. Since 2000, there has been an explosion of interest in negative refraction [1, 2], following experimental reports of a metamaterial which supports negative refraction in the microwave regime [3].

Naturally-occurring uniaxial crystals have been extensively studied ever since the earliest days of the optical sciences. However, the electromagnetic properties of uniaxial mediums have recently been revisited by theoreticians in consideration of the prospects for NPV propagation in such mediums [4, 5, 6, 7]. A closely related issue concerns uniaxial dielectric-magnetic mediums with indefinite constitutive dyadics [8, 9].

The defining characteristic of a uniaxial dielectric medium is a distinguished axis of symmetry, known as the optic axis. Mathematically, the permittivity dyadic of a uniaxial dielectric medium may be expressed as

$$\underline{\underline{\epsilon}} = \epsilon \underline{\underline{I}} + (\epsilon_x - \epsilon) \hat{x} \hat{x}, \quad (1)$$

where a coordinate system has been selected in which the direction of the optic axis coincides with the direction of the unit vector \hat{x} lying along the x axis, and $\underline{\underline{I}}$ denotes the 3×3 identity dyadic. The real-valued parameter

$$\gamma = \begin{cases} \frac{\epsilon_x}{\epsilon} & \text{for } \epsilon_x, \epsilon \in \mathbb{R} \\ \frac{\text{Re}\{\epsilon_x\}}{\text{Re}\{\epsilon\}} & \text{for } \epsilon_x, \epsilon \in \mathbb{C} \end{cases} \quad (2)$$

may be usefully employed to characterize planewave propagation in the medium specified by (1). The upper expression is appropriate to nondissipative mediums whereas the lower expression is appropriate to dissipative mediums.

The electromagnetic/optical properties of uniaxial mediums with $\gamma > 0$ — this category includes naturally-occurring uniaxial crystals — have long been established. Comprehensive descriptions can be found in standard works [10, 11]. Uniaxial mediums with $\gamma < 0$ are much more exotic. Interest in these mediums stems from their potential applications in negatively refracting scenarios [8, 9] and in diffraction gratings [12], for example.

Planewave propagation in a uniaxial medium is characterized in terms of a dispersion relation which is quadratic in terms of the corresponding wavevector components. The dispersion relations for nondissipative mediums with $\gamma > 0$ have an elliptical representation, whereas a hyperbolic representation is associated with $\gamma < 0$. In this communication we investigate the planewave characteristics and conceptualization of uniaxial dielectric mediums with hyperbolic dispersion relations.

2 Planewave analysis

The propagation of plane waves with field phasors

$$\left. \begin{aligned} \underline{E}(\underline{r}) &= \underline{E}_0 \exp(i\underline{k} \cdot \underline{r}) \\ \underline{H}(\underline{r}) &= \underline{H}_0 \exp(i\underline{k} \cdot \underline{r}) \end{aligned} \right\} \quad (3)$$

in the uniaxial dielectric medium specified by the permittivity dyadic (1) is investigated. The permittivity parameters are generally complex-valued; i.e., $\epsilon, \epsilon_x \in \mathbb{C}$. The wavevector \underline{k} is taken to be of the form

$$\underline{k} = \alpha \hat{x} + \beta \hat{z}, \quad (4)$$

where $\alpha \in \mathbb{R}$, $\beta \in \mathbb{C}$ and \hat{z} is the unit vector directed along the z axis. This form of \underline{k} is appropriate to planar boundary value problems [11] and from the practical viewpoint of potential optical devices [12]. We note that the plane waves (3) are generally nonuniform.

The source-free Maxwell curl postulates

$$\left. \begin{aligned} \nabla \times \underline{E}(\underline{r}) &= i\omega \underline{B}(\underline{r}) \\ \nabla \times \underline{H}(\underline{r}) &= -i\omega \underline{D}(\underline{r}) \end{aligned} \right\} \quad (5)$$

yield the vector Helmholtz equation

$$\left[(\nabla \times \underline{I}) \cdot (\nabla \times \underline{I}) - \mu_0 \omega^2 \underline{\epsilon} \right] \cdot \underline{E}(\underline{r}) = \underline{0}, \quad (6)$$

with μ_0 being the permeability of free space. Combining (3) with (6) yields the planewave dispersion relation

$$(\alpha^2 + \beta^2 - \epsilon \mu_0 \omega^2) (\alpha^2 \epsilon_x + \beta^2 \epsilon - \epsilon_x \epsilon \mu_0 \omega^2) = 0. \quad (7)$$

In the following we consider the time-averaged Poynting vector

$$\underline{P}(\underline{r}) = \frac{\exp(-2 \operatorname{Im}\{\beta\} z)}{2\mu_0 \omega} \operatorname{Re} \left\{ |\underline{E}_0|^2 \underline{k}^* - (\underline{E}_0 \cdot \underline{k}^*) \underline{E}_0^* \right\}. \quad (8)$$

Evanescent plane waves are characterized by $\operatorname{Im}\{\beta\} > 0$. The scenario characterized by $\operatorname{Im}\{\beta\} < 0$ is not physically plausible for passive mediums and is therefore not considered here.

2.1 Ordinary wave

The ordinary wavevector

$$\underline{k}_{or} = \alpha \hat{x} + \beta_{or} \hat{z}, \quad (9)$$

arises from the dispersion relation (7) with components satisfying

$$\alpha^2 + \beta_{or}^2 = \omega^2 \epsilon \mu_0. \quad (10)$$

The vector Helmholtz equation (6) yields the eigenvector solution $\underline{E}_0 = E_y \hat{y}$, directed parallel to the unit vector \hat{y} lying along the y axis, where the complex-valued magnitude E_y is determined by the initial/boundary conditions. Consequently, the time-averaged Poynting vector reduces to

$$\underline{P}(\underline{r}) = \frac{\exp(-2 \operatorname{Im}\{\beta_{or}\} z)}{2\omega\mu_0} |E_y|^2 \operatorname{Re}\{\underline{k}_{or}^*\}. \quad (11)$$

Since

$$\operatorname{Re}\{\underline{k}_{or}\} \cdot \underline{P}(\underline{r}) = \frac{\exp(-2 \operatorname{Im}\{\beta_{or}\} z)}{2\omega\mu_0} |E_y|^2 [\alpha^2 + (\operatorname{Re}\{\beta_{or}\})^2] \geq 0, \quad (12)$$

we say that ordinary plane waves have positive phase velocity (PPV) for all directions of propagation.

Let us focus attention on a nondissipative medium (i.e., $\epsilon, \epsilon_x \in \mathbb{R}$). From (10) we see that $\operatorname{Im}\{\beta_{or}\} \neq 0$ for (i) $\epsilon > 0$ when $\omega^2\epsilon\mu_0 < \alpha^2$; and (ii) $\epsilon < 0$. Thus, nonevanescant ordinary plane waves propagate in a nondissipative medium only when $\epsilon > 0$ and $-\omega\sqrt{\epsilon\mu_0} < \alpha < \omega\sqrt{\epsilon\mu_0}$. In geometric terms, the wavevector components have a circular representation in (α, β_{or}) space.

2.2 Extraordinary wave

The extraordinary wavevector

$$\underline{k}_{ex} = \alpha \hat{x} + \beta_{ex} \hat{z}, \quad (13)$$

arises from the dispersion relation (7) with components satisfying

$$\alpha^2\epsilon_x + \beta_{ex}^2\epsilon = \omega^2\epsilon\epsilon_x\mu_0. \quad (14)$$

In the case where $\beta_{ex} = 0$ the mathematical description of the extraordinary wave is isomorphic to that for the ordinary wave. Therefore, we exclude this possibility from our consideration in this section. The eigenvector

$$\underline{E}_0 = \left(\hat{x} - \frac{\epsilon_x \alpha}{\epsilon \beta_{ex}} \hat{z} \right) E_x, \quad (15)$$

arises as a solution to the vector Helmholtz equation (6); the complex-valued magnitude E_x is determined by the initial/boundary conditions. The corresponding time-averaged Poynting vector is provided as

$$\begin{aligned} \underline{P}(\underline{r}) = & \frac{\exp(-2 \operatorname{Im}\{\beta_{ex}\} z)}{2\omega\mu_0} \operatorname{Re} \left\{ \alpha \left(\left| \frac{\epsilon_x}{\epsilon \beta_{ex}} \right|^2 \alpha^2 + \frac{\epsilon_x \beta_{ex}^*}{\epsilon \beta_{ex}} \right) \hat{x} \right. \\ & \left. + \left(\beta_{ex}^* + \alpha^2 \frac{\epsilon_x^*}{\epsilon^* \beta_{ex}^*} \right) \hat{z} \right\} |E_x|^2. \end{aligned} \quad (16)$$

Hence, we find

$$\begin{aligned} \text{Re}\{k_{ex}\} \cdot \underline{P}(\underline{r}) &= \frac{\exp(-2 \text{Im}\{\beta_{ex}\}z)}{2\omega\mu_0} \left[(\text{Re}\{\beta_{ex}\})^2 \right. \\ &\quad \left. + \alpha^2 \left(\alpha^2 \left| \frac{\epsilon_x}{\epsilon\beta_{ex}} \right|^2 + \text{Re}\left\{ \frac{\epsilon_x\beta_{ex}^*}{\epsilon\beta_{ex}} \right\} + \text{Re}\{\beta_{ex}\} \text{Re}\left\{ \frac{\epsilon_x^*}{\epsilon^*\beta_{ex}^*} \right\} \right) \right]. \end{aligned} \quad (17)$$

We analytically explore the nondissipative scenario for nonevanescant and evanescent planewave propagation in Sections 2.3 and 2.4, respectively, whereas both the dissipative and the nondissipative scenarios are treated graphically in Section 2.5.

2.3 Nonevanescant propagation

By (14), the inequality

$$\omega^2\epsilon_x\mu_0 - \alpha^2\gamma > 0 \quad (18)$$

is satisfied for nonevanescant planewave propagation in a nondissipative medium, where γ is defined in (2). Thus, $\text{Im}\{\beta_{ex}\} = 0$. We explore the cases $\gamma > 0$ and $\gamma < 0$ separately.

- (i) If $\gamma > 0$ then we require $-\omega\sqrt{\epsilon\mu_0} < \alpha < \omega\sqrt{\epsilon\mu_0}$ in order to comply with (18). This implies that $\epsilon > 0$ and $\epsilon_x > 0$. In geometric terms, the wavevector components have an elliptical representation in (α, β_{ex}) space.
- (i) If $\gamma < 0$ then the inequality (18) reduces to $\omega^2\epsilon\mu_0 < \alpha^2$. Therefore, we see that nonevanescant propagation arises for (a) $\alpha > \omega\sqrt{\epsilon\mu_0}$ and $\alpha < -\omega\sqrt{\epsilon\mu_0}$ when $\epsilon > 0$; and (b) $-\infty < \alpha < \infty$ when $\epsilon < 0$. In geometric terms, the wavevector components have a hyperbolic representation in (α, β_{ex}) space.

For $\text{Im}\{\beta_{ex}\} = 0$ and $\epsilon_x, \epsilon \in \mathbb{R}$, we find that (17) reduces to

$$\text{Re}\{k_{ex}\} \cdot \underline{P}(\underline{r}) = \frac{\omega^3\mu_0\gamma^2\epsilon_x^2}{2\beta_{ex}^2}. \quad (19)$$

Hence, nonevanescant plane waves have PPV regardless of the sign of γ or ϵ_x .

2.4 Evanescent propagation

We turn to evanescent planewave propagation in a nondissipative medium as characterized by the inequality

$$\omega^2\epsilon_x\mu_0 - \alpha^2\gamma < 0. \quad (20)$$

Hence, we have $\text{Re}\{\beta_{ex}\} = 0$. As in the previous subsection, we explore the cases $\gamma > 0$ and $\gamma < 0$ separately.

- (i) If $\gamma > 0$ then the situation mirrors that which we described earlier for hyperbolic nonevanescant propagation. That is, evanescent propagation arises for (a) $\alpha > \omega\sqrt{\epsilon\mu_0}$ and $\alpha < -\omega\sqrt{\epsilon\mu_0}$ when $\epsilon > 0$; and (b) $-\infty < \alpha < \infty$ when $\epsilon < 0$. In geometric terms, the wavevector components have a hyperbolic representation in $(\alpha, \text{Im}\{\beta_{ex}\})$ space.
- (ii) If $\gamma < 0$ then evanescent propagation arises provided that $\epsilon > 0$, $\epsilon_x < 0$ and $-\omega\sqrt{\epsilon\mu_0} < \alpha < \omega\sqrt{\epsilon\mu_0}$. In geometric terms, the wavevector components have an elliptical representation in $(\alpha, \text{Im}\{\beta_{ex}\})$ space.

For $\text{Re}\{\beta_{ex}\} = 0$ and $\epsilon_x, \epsilon \in \mathbb{R}$, we find that (17) reduces to

$$\text{Re}\{\underline{k}_{ex}\} \cdot \underline{P}(\underline{r}) = \frac{\omega\alpha^2\epsilon_x\gamma}{2(\alpha^2\gamma - \omega^2\mu_0\epsilon_x)} \exp(-2\text{Im}\{\beta_{ex}\}z). \quad (21)$$

Hence, evanescent plane waves have PPV if (a) $\gamma < 0$ or (b) $\gamma > 0$ and $\epsilon_x > 0$. However, negative phase velocity (NPV) propagation arises if $\gamma > 0$ and $\epsilon_x < 0$.

2.5 Illustrative examples

Let us illustrate the geometric aspect of the dispersion relations with some representative numerical examples.

First, suppose we consider the case $\gamma > 0$ with $\epsilon = 2\epsilon_0$ and $\epsilon_x = 6\epsilon_0$, where ϵ_0 is the free-space permittivity. In Figure 1 the real and imaginary parts of β_{ex} are plotted against α . The elliptical nonevanescant nature of the dispersion relation is clear for $-\omega\sqrt{2\epsilon_0\mu_0} < \alpha < \omega\sqrt{2\epsilon_0\mu_0}$, while the hyperbolic evanescent nature is apparent for $\alpha < -\omega\sqrt{2\epsilon_0\mu_0}$ and $\alpha > \omega\sqrt{2\epsilon_0\mu_0}$. The elliptical/hyperbolic geometric interpretation breaks down when dissipative mediums are considered. However, the corresponding dispersion relations are geometrically reminiscent of their nondissipative counterparts. This can be observed in Figure 2 in which the graphs corresponding to Figure 1 are displayed for $\epsilon = (2 + i0.5)\epsilon_0$ and $\epsilon_x = (6 + i0.75)\epsilon_0$.

Second, we turn to the case $\gamma < 0$ with $\epsilon = 2\epsilon_0$ and $\epsilon_x = -6\epsilon_0$. The real and imaginary parts of β_{ex} are graphed against α in Figure 3. The graphs mirror those of Figure 1 but with nonevanescant and evanescent aspects interchanged; i.e., we observe hyperbolic nonevanescant characteristics for $\alpha < -\omega\sqrt{2\epsilon_0\mu_0}$ and $\alpha > \omega\sqrt{2\epsilon_0\mu_0}$, and elliptical evanescent characteristics for $-\omega\sqrt{2\epsilon_0\mu_0} < \alpha < \omega\sqrt{2\epsilon_0\mu_0}$. The corresponding graphs for $\epsilon = (2 + i0.5)\epsilon_0$ and $\epsilon_x = (-6 + i0.75)\epsilon_0$ are presented in Figure 4. Notice that the shapes of the graphs in Figures 4 and 2 are similar but not identical.

3 Numerical conceptualization

Although uniaxial dielectric mediums with $\gamma < 0$ do not occur in nature (to the best of the authors' knowledge), they can be conceptualized as metamaterials by means of homogenization.

For example, let us consider the homogenization of a composite comprising two component materials phases, labelled as a and b . Both component material phases are taken to be isotropic dielectric mediums: ϵ^a and ϵ^b denote the permittivity scalars of phases a and b , respectively. The component material phases are envisioned as random distributions of identically-oriented, spheroidal particles. The spheroidal shape — which is taken to be the same for all spheroids in component material phase a and b — is parameterized via the shape dyadic $\underline{\underline{U}} = \text{diag}(U_x, U, U)$. That is, we take the spheroid's principal axis to lie along the x axis. The spheroid's surface is prescribed by the vector

$$\underline{r}_s(\theta, \phi) = \eta \underline{\underline{U}} \cdot \hat{\underline{r}}(\theta, \phi), \quad (22)$$

with $\hat{\underline{r}}$ being the radial unit vector specified by the spherical polar coordinates θ and ϕ . The linear dimensions of the spheroid, as determined by the parameter η , are assumed to be small relative to the electromagnetic wavelength(s).

The permittivity dyadic of the resulting homogenized composite medium (HCM)

$$\underline{\underline{\epsilon}}^{HCM} = \text{diag}(\epsilon_x^{HCM}, \epsilon^{HCM}, \epsilon^{HCM}), \quad (23)$$

as estimated using the Bruggeman homogenization formalism, is provided implicitly via

$$f_a \underline{\underline{a}}^a + f_b \underline{\underline{a}}^b = \underline{\underline{0}}, \quad (24)$$

where f_a and $f_b = 1 - f_a$ denote the respective volume fractions of the material component phases a and b . The polarizability dyadics in (24) are defined as

$$\underline{\underline{a}}^\ell = (\epsilon^\ell \underline{\underline{I}} - \underline{\underline{\epsilon}}^{HCM}) \cdot [\underline{\underline{I}} + i\omega \underline{\underline{D}} \cdot (\epsilon^\ell \underline{\underline{I}} - \underline{\underline{\epsilon}}^{HCM})]^{-1}, \quad (\ell = a, b), \quad (25)$$

wherein the depolarization dyadic is given by the surface integral

$$\underline{\underline{D}} = \frac{1}{i\omega 4\pi} \int_0^{2\pi} d\phi \int_0^\pi d\theta \sin \theta \left(\frac{1}{\hat{\underline{r}} \cdot \underline{\underline{U}}^{-1} \cdot \underline{\underline{\epsilon}}^{HCM} \cdot \underline{\underline{U}}^{-1} \cdot \hat{\underline{r}}} \right) \underline{\underline{U}}^{-1} \cdot \hat{\underline{r}} \hat{\underline{r}} \cdot \underline{\underline{U}}^{-1}. \quad (26)$$

Closed-form expressions for the depolarization dyadic for uniaxial mediums are available in terms of hyperbolic functions [15]. However, we note that these exact results are not valid for nondissipative mediums with $\gamma < 0$, and numerical evaluation of $\underline{\underline{D}}$ has to be resorted to.

The Jacobi iteration scheme

$$\underline{\underline{\epsilon}}^{HCM}[p] = \mathcal{T} \{ \underline{\underline{\epsilon}}^{HCM}[p-1] \}, \quad (p = 1, 2, 3, \dots), \quad (27)$$

where the operator \mathcal{T} is defined via

$$\begin{aligned} \mathcal{T} \{ \underline{\underline{\epsilon}}^{HCM} \} = & \left\{ f_a \epsilon^a [\underline{\underline{I}} + i\omega \underline{\underline{D}} \cdot (\epsilon^a \underline{\underline{I}} - \underline{\underline{\epsilon}}^{HCM})]^{-1} + f_b \epsilon^b [\underline{\underline{I}} + i\omega \underline{\underline{D}} \cdot (\epsilon^b \underline{\underline{I}} - \underline{\underline{\epsilon}}^{HCM})]^{-1} \right\} \\ & \cdot \left\{ f_a [\underline{\underline{I}} + i\omega \underline{\underline{D}} \cdot (\epsilon^a \underline{\underline{I}} - \underline{\underline{\epsilon}}^{HCM})]^{-1} + f_b [\underline{\underline{I}} + i\omega \underline{\underline{D}} \cdot (\epsilon^b \underline{\underline{I}} - \underline{\underline{\epsilon}}^{HCM})]^{-1} \right\}^{-1}, \end{aligned} \quad (28)$$

may be employed to solve (24) for $\underline{\underline{\epsilon}}^{HCM}$. Suitable initial values for the iterative scheme are provided by

$$\underline{\underline{\epsilon}}^{HCM}[0] = (f_a \epsilon^a + f_b \epsilon^b) \underline{\underline{I}}. \quad (29)$$

For further details on the Bruggeman homogenization formalism the reader is referred to [13, 14] and to references therein.

Let us consider the homogenization scenario wherein material component phase a is taken to be iron at 670 nm free-space wavelength. Correspondingly, we take $\epsilon^a = (-4.34 + i20.5) \epsilon_0$. The material component phase b is assumed to be free space; i.e., $\epsilon^b = \epsilon_0$. The shape of the component spheroids is specified by $U_x/U = 12$. The Bruggeman estimates of the HCM permittivity parameters ϵ^{HCM} and ϵ_x^{HCM} are plotted as functions of volume fraction f_a in Figure 5. At intermediate values of f_a we see that $\gamma < 0$ for a substantial range of f_a values.

Extensive accounts of similar numerical homogenizations, based on the Bruggeman formalism and more general approaches, can be found elsewhere [13, 16].

4 Concluding remarks

The dispersion relations for uniaxial dielectric mediums have been characterized with respect to the parameter γ (2). For $\gamma < 0$, the dispersion relations are hyperbolic for nondissipative mediums and hyperbolic-like for dissipative mediums. Similarly, the dispersion relations are elliptical for nondissipative mediums and elliptical-like for dissipative mediums with $\gamma > 0$. Through the homogenization of isotropic component material phases based on spheroidal topology, we demonstrate that metamaterials with $\gamma < 0$ may be straightforwardly conceptualized. Thus, a practical means of achieving the exotic electromagnetic properties associated with hyperbolic and hyperbolic-like uniaxial mediums is presented.

References

- [1] Pendry J B 2004 Negative refraction *Contemp. Phys.* **45** 191–202
- [2] Ramakrishna S A 2005 Physics of negative refractive index materials *Rep. Progr. Phys.* **68** 449–521
- [3] Shelby R A, Smith D R and Schultz S 2001 Experimental verification of a negative index of refraction *Science* **292** 77–79
- [4] Kärkkäinen M K 2003 Numerical study of wave propagation in uniaxially anisotropic Lorentzian backward-wave slabs *Phys. Rev. E* **68** 026602
- [5] Liu Z, Xu J and Lin Z 2004 Omnidirectional reflection from a slab of uniaxially anisotropic negative refractive index materials *Opt. Commun.* **240** 19–27
- [6] Yonghua L, Pei W, Peijun Y, Jianping X and Hai M 2005 Negative refraction at the interface of uniaxial anisotropic media *Opt. Commun.* **246** 429–435

- [7] Perez L I, Garea M T and Echarri R M 2005 Isotropic–uniaxial crystal interfaces: negative refraction and backward wave phenomena *Opt. Commun.* (at press)
- [8] Smith D R and Schurig D 2003 Electromagnetic wave propagation in media with indefinite permittivity and permeability tensors *Phys. Rev. Lett.* **90** 077405
- [9] Smith D R, Kolinko P and Schurig D 2004 Negative refraction in indefinite media *J. Opt. Soc. Am. B* **21** 1032–1043
- [10] Born M and Wolf E 1980 *Principles of Optics, 6th ed* (Oxford: Pergamon)
- [11] Chen H C 1983 *Theory of Electromagnetic Waves* (New York: McGraw–Hill)
- [12] Depine R A and Lakhtakia A 2005 Diffraction by a grating made of a uniaxial dielectric–magnetic medium exhibiting negative refraction *New J. Physics* (accepted for publication)
- [13] Sherwin J A, Lakhtakia A and Michel B 2000 Homogenization of similarly oriented, metallic, ellipsoidal inclusions using the Bruggeman formalism *Opt. Commun.* **178** 267–273
- [14] Mackay T G 2003 Homogenization of linear and nonlinear complex composite materials *Introduction to Complex Mediums for Optics and Electromagnetics* ed WS Weiglhofer and A Lakhtakia (Bellingham, WA: SPIE Press) pp317–345
- [15] Michel B 1997 A Fourier space approach to the pointwise singularity of an anisotropic dielectric medium *Int. J. Appl. Electromag. Mech.* **8** 219–227
- [16] Mackay T G, Lakhtakia A and Weiglhofer W S 2001 Homogenisation of similarly oriented, metallic, ellipsoidal inclusions using the bilocally approximated strong–property–fluctuation theory *Opt. Commun.* **197** 89–95

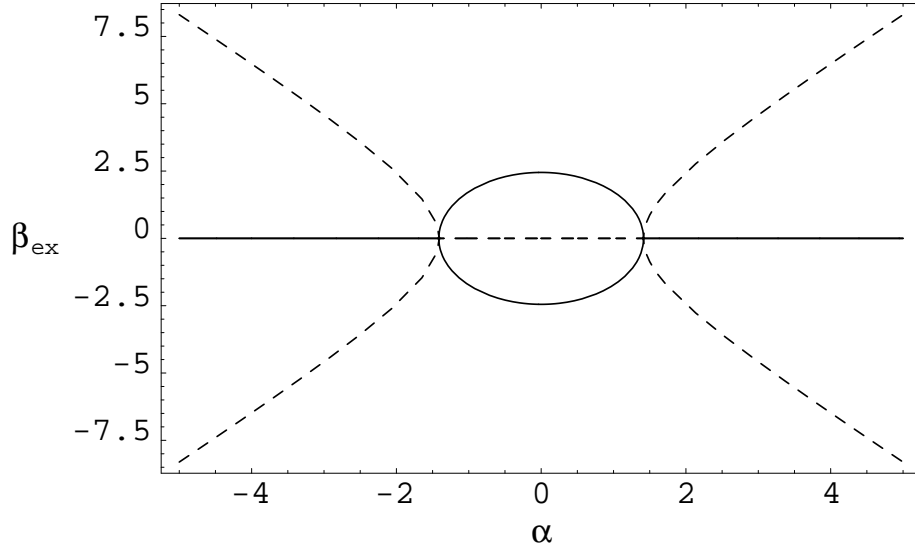


Figure 1: A plot of the real (solid curve) and imaginary (dashed curve) parts of β_{ex} against α for $\epsilon_x = 6\epsilon_0$ and $\epsilon = 2\epsilon_0$. The values of α and β_{ex} are normalized with respect to $\omega\sqrt{\epsilon_0\mu_0}$.

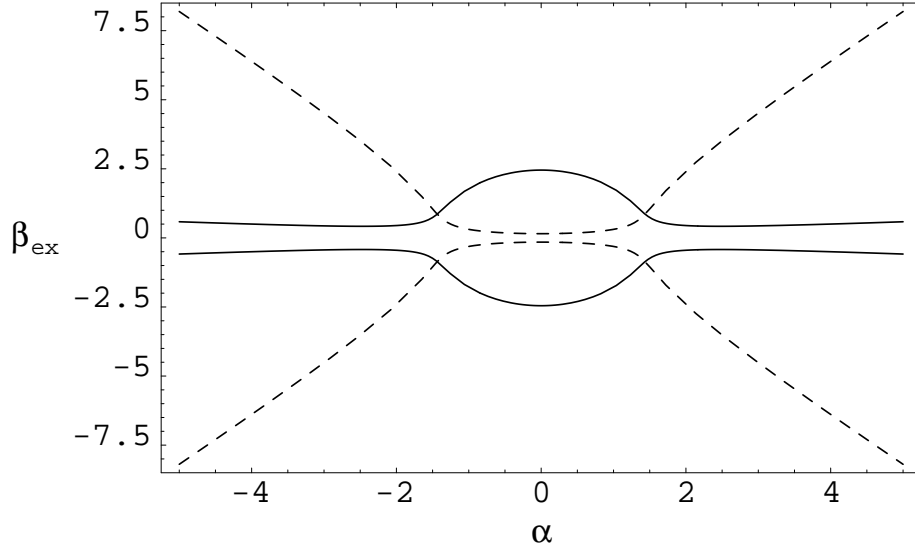


Figure 2: As figure 1 but for $\epsilon_x = (6 + i0.75)\epsilon_0$ and $\epsilon = (2 + i0.5)\epsilon_0$.

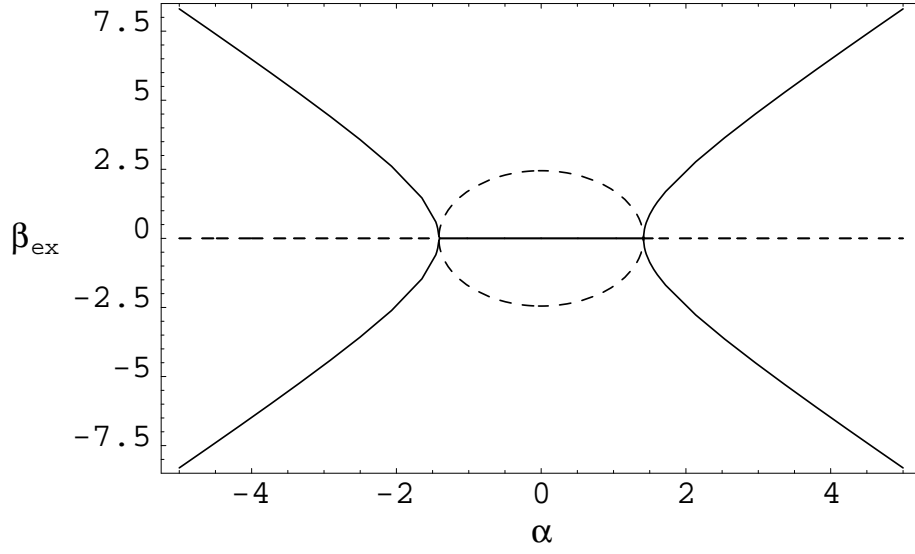


Figure 3: A plot of the real (solid curve) and imaginary (dashed curve) parts of β_{ex} against α for $\epsilon_x = -6\epsilon_0$ and $\epsilon = 2\epsilon_0$. The values of α and β_{ex} are normalized with respect to $\omega\sqrt{\epsilon_0\mu_0}$.

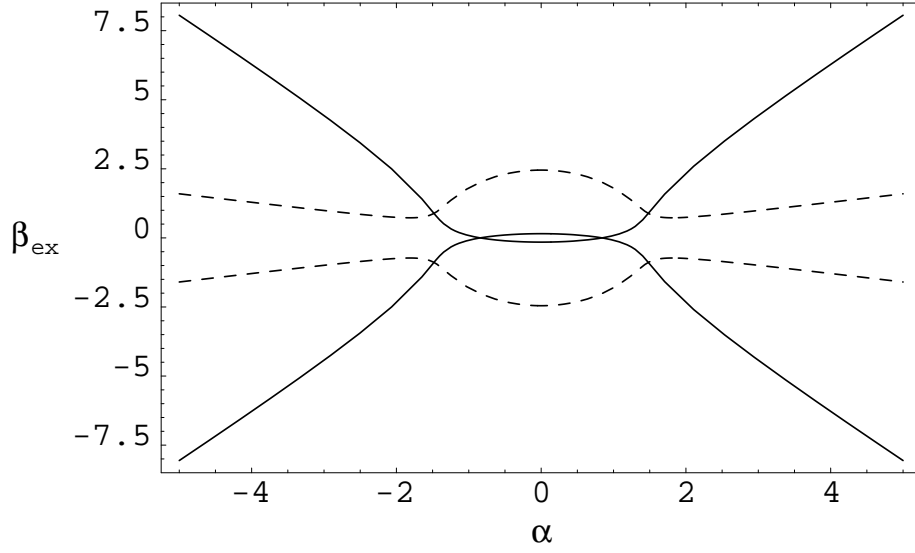


Figure 4: As figure 3 but for $\epsilon_x = (-6 + i0.75)\epsilon_0$ and $\epsilon = (2 + i0.5)\epsilon_0$.

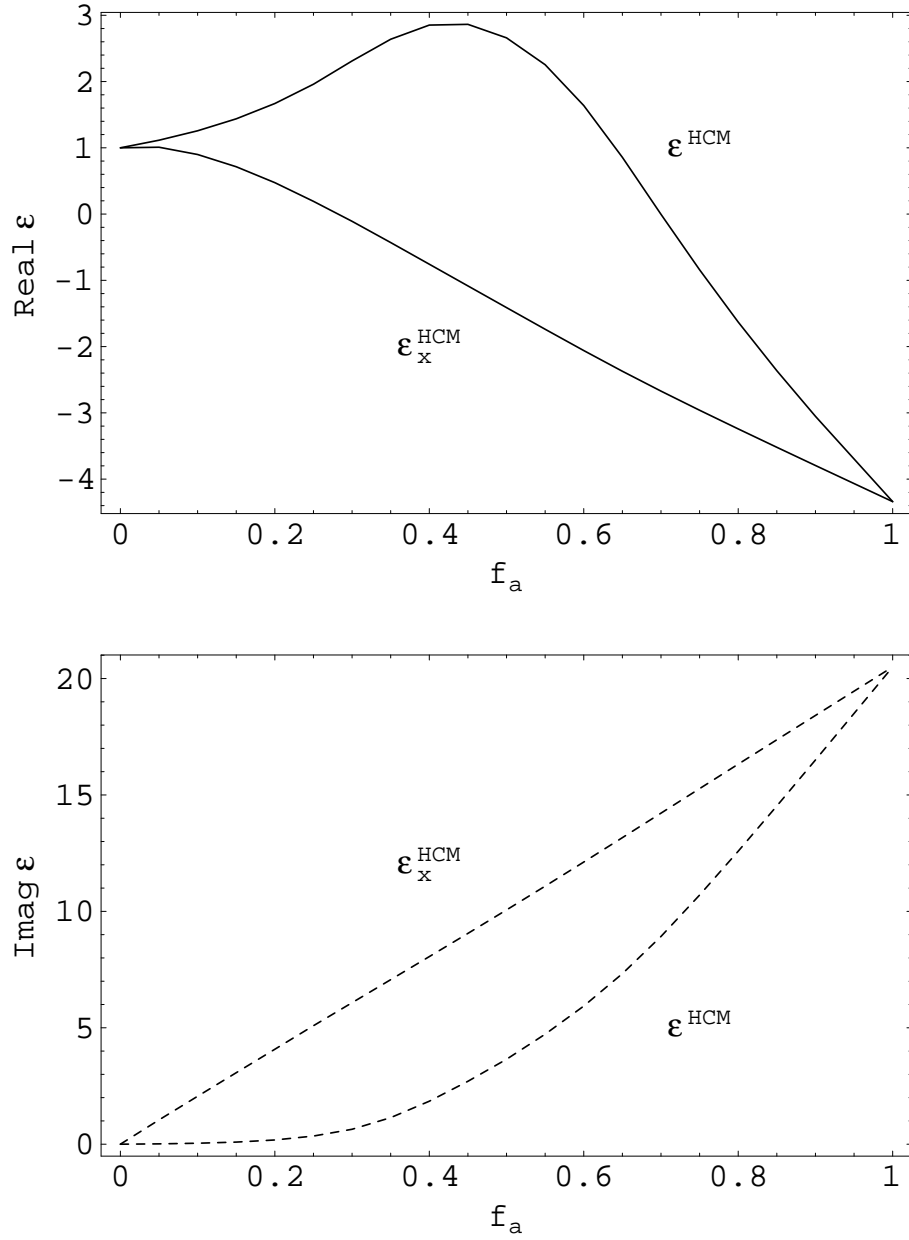


Figure 5: The real (above) and imaginary (below) parts of ϵ^{HCM} and ϵ_x^{HCM} plotted against volume fraction f_a . The permittivity values are normalized with respect to ϵ_0 . Component phase values: $\epsilon^a = (-4.34 + i20.5)\epsilon_0$ and $\epsilon^b = \epsilon_0$; spheroidal shape parameters: $U_x/U = 12$.